# The use of AA7075-T651 Alloy in Combat Vehicles Offers Superior Properties Compared to Steel, Providing Enhanced Strength and Durability: A Review

Amal C. Kumar[1*], Abey Vishnu Narayana[2]

[1]Department of Mechanical Engineering Snit Adoor

[2]Assistant Professor Department of Mechanical Engineering Snit Adoor

*Corresponding author's e-mail: amalck2251@gmail.com

doi: https://doi.org/10.21467/proceedings.160.61

**ABSTRACT**

Friction stir welding (FSW) is a solid-state welding method that is widely used in industries such as aerospace and automotive. It is particularly effective in joining non-heat-treatable aluminium alloys like the 3xxx and 5xxx series, as well as the heat-treatable 7075 aluminium alloy. The 7075 alloy, developed by Alcoa in 1943, is composed of copper, zinc, magnesium, chromium, and small amounts of other elements. It exhibits high strength after undergoing a heat treatment process, surpassing that of many other aluminium alloys. Different temper designations, such as 7075-T-6, T-651, T-7351, T-73, T-76, T-7651, and W5-1, guide the use of the 7075 alloy. In this study, the focus was on the resistance of 25-millimetre-thick plates made of AA7075-T651 (a specific form of the 7075 alloy) to penetration by two types of projectiles. The base material and all three zones of the welded plates (weld nugget, heat-affected zone, and thermo-mechanically affected zone) showed resistance to penetration. Steel core bullets exhibited better penetration than lead core projectiles. The thermo-mechanically affected zone (TMAZ) was found to be the weakest region after friction stir welding, with signs of fracture including splinter fragmentation in the base material and front petalling in all zones of the welded plates. Microstructural analysis revealed no significant changes in the base material and weld nugget after the ballistic experiment. However, the TMAZ and heat-affected zone showed the formation of adiabatic shear bands, indicating localized deformation due to projectile impact. Overall, the study demonstrated that 25-millimetre-thick friction stir-welded AA7075-T651 intersections exhibited excellent performance under ballistic impact loads. This suggests that FSW could be a promising option for lightweight combat boats, providing increased strength and protection. These joints could also be beneficial for defence vehicles in various applications.

**Keywords:** Friction stir welding, AA7075-T651 alloy plates, Depth of penetration

## 1 Introduction

Metals are usually second-hand in armour design for their talent to support effective care while bearing structural and fatigue loads. Steel has ordinarily happened the primary silvery material second-hand in bulletproof combat vehicles for justification [1]. However, in current decades, researchers have been attracted to inconsequential materials accompanying impact opposition for fabricating protective forms in combat automobiles. Titanium, magnesium, and usually metallic have emerged as appropriate substitutes to steel on account of their reduced areal mass, extreme substance-to-weight percentage, and benign mechanical, material, and warm properties. While titanium and magnesium offer benefits in the way that lightness and reduced mass, the extreme cost of titanium and the self-ignition risk of magnesium pose meaningful challenges [2]. As a result, usually metallic and its alloys have enhanced adjustable options for shield planners [3]. Aluminium alloys, with their depressed mass and pliable properties varying from 60 to 600 MPa, be worthwhile for providing greater capacity for an equal bulk compared to brace, so enhancing the severity of bulletproof forms [4]. Among the rolled and extreme-substance aluminium alloys, AA7075



Proceedings DOI: 10.21467/proceedings.160; Series: AIJR Proceedings; ISSN: 2582-3922; ISBN: 978-81-965621-9-9

is conspicuous as a hopeful alternative to steel shields on account of its extreme strength-engrossing capabilities and strength-weight ratio.

The age- or hard enable order of AA7075 metals is prone to passionate breaking and mis-spreading the heat-affected zones all along mixture binding, particularly because of the solid law enforcement officer content (1.75 wt%) [5]. This rooftop using binding methods is contradictory with the age-hardenable order of AA7075 metals [6]. However, the hard-state ore touching process, known as FSW, has favourably joined as a rule unweldable usually metallic alloys to a degree Al-Cu and Al, Zn, Mg, Cu series alloys [7]. FSW offers many benefits, containing flawless welds, good fundamental security, and the skill to find weld intersections accompanying miscellaneous profiles, and prime junctures. During disagreement stir welding, meaningful flexible deformity, frictional heat, and hardware flow occur on account of the moving operation of the tool [8]. The hotness in the welded fields rises to 420 to 480°C, forestalling melting as it debris beneath the softening hotness of 80% [9]. FSW exhibit four distinct zones: the base material, thermo-automatically jolted district, weld lump district, and heat-impressed zone. Strengthening precipitates in the welded intersections discontinue on account of the frictional heat, resulting in the softening of the material and belittled machinelike traits [10].

Several studies have checked the mechanical and microstructural action of FSW AA7075-T651 plates accompanying different process limits [11]. These studies have examined the pliable properties, severity, disintegration fighting, impacts of post-connect treatments, and microstructural changes in rubbing stir-welded container alloy AA7075. However, the denseness of the plates analysed in these studies was categorized from 4 to 16 million metres, and no particular consideration was given to 25 milli metre-dense rubbing stir welded AA7075-T651 goals [12].

Ballistic opposition in fabrics is influenced by determinants in the way that surface severity, yield strength, regional bulk, impact determination, shear substance, and strength-absorptive capability. The accomplishment of fabrics in ballistics tests evaluated established determinants to a degree penetration wisdom of the bullet, way of failure, flexible deformity familiar with the impact site, and opposition to shock waves produce by unexpected impact.

Several studies have explored the ballistic management of resistance stir-treated targets, differing base material grades, moderating hotnesses, and friction stir connecting of finer goals. However, there have happened no attempts to study the machinelike properties and ballistic act of 25 milli metre-dense FSW AA7075-T651 aims [13]. In this study, the ballistic conduct of targets against 7.62 milli metre lead gist and brace centre rounds at different impact velocities was checked in miscellaneous zones.

## 2 Material Used and Methodology

In the study, 25 milli metre dense AA7075-T651 rolled plates were second-hand as the base material for friction stir welding. The connecting finish used was made from M2 form gird. The basic dispersion of the base material is bestowed in Table 1. X-ray range studies were attended not completely three periods to acquire the presented values. Friction stir connecting was acted on base material plates weighing 150 milli metre in breadth and 300 milli metre in time [14]. The plates were longitudinally butt-welded utilizing resistance stir connecting supplies.

**Table 1**: *The composition of the material in weight percentage.*

| Material | Zn | Mg | Cu | Cr | Fe | Ti | Si | Mn | Al |
|---|---|---|---|---|---|---|---|---|---|
| AA7075 | 6.0 | 2.5 | 1.4 | 0.20 | 0.08 | 0.05 | 0.03 | 0.01 | 89.73 |

Proceedings DOI: 10.21467/proceedings.160
ISBN: 978-81-965621-9-9

Series: AIJR Proceedings
ISSN: 2582-3922

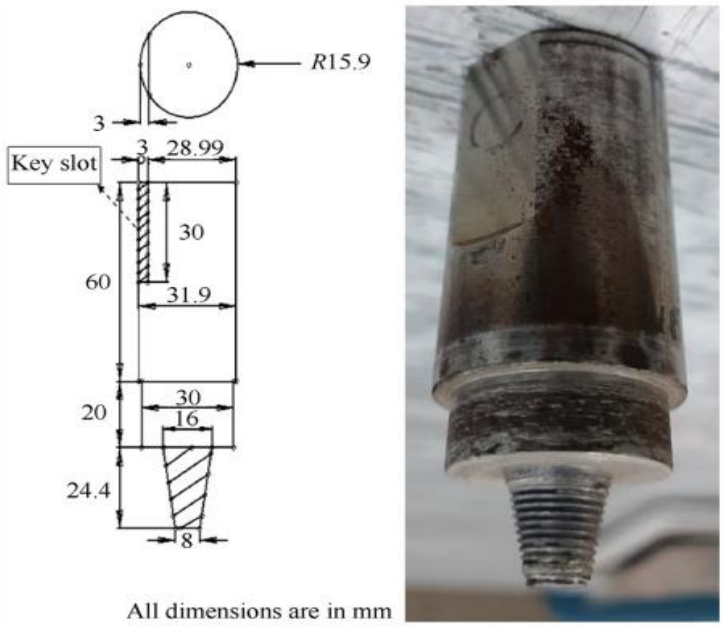


**Figure 1:** *Showcases the FSW tool used to create 25-million metre-thick welds*

In this study, a usual resistance stir connecting mechanism was utilized for building welds. The fs welds were acted on 25 milli metre AA7075-T651 plates utilizing an abandoned-help intertwine, tapered attach characterization (truncated cone) to prevent root osculation bond [15]. Table 2 supports details of the finish arithmetic and process variables that were deliberate for the inquiry. These limits were painstakingly selected through diversified redundancies to solve alone-pass, defect-free, complete-infiltration, weld accompanying a concave fundamental stir positions [16]. Vickers microhardness calculations were attended at the connect cross-intervening-thickness domain, administering a 0.5 kg force and a 10 s reside period.

For the pliable experiment, samples were taken from the transverse route to the connected home, following the ASTM B557M standard [17]. Figure 4(a) demonstrates the ranges of a diagram 2D pliable sample, while Figure 4(b) shows fracture samples.

Charpy impact tests were acted by ASTM E23. The base material's disagreement stir bind and ballistics tests were transported similarly to defence necessities particularized by NIJ.0108.01[18]. Figures 2(a) and 2(b) describe a diagram of exploratory ballistic test arrangement and an attractive view of an automated mortar drum original, individually. Projectiles accompanying 7.62 milli metre × 51 milli metre lead gist and 7.62 milli metre × 39 milli metre hard steel gist were proven on the base material and rubbing stir welded plates of 25 milli metre density and 300 milli metre in intensity [19]. Images of the bullets are shown in Figures 3(a) and 3(b). During the whole experiment process, the lead gist bullets were admitted to contacting at a full speed of 830 ± 20 m/s, while the gird core bullets were admitted to contacting at a full speed of 700 ± 30 m/s. Impact velocities in each trial were calculated utilizing specific velocity calculation supplies, and the bullets were discharged from a 10 m distance.

Metallurgical reasoning of the resistance stir welded plates was conducted utilizing two an ocular light microscope and a broadcast energized matter microscope. Samples for the ocular microscope study were taken from all bind zones by particularized ranges. The samples were refined utilizing a comically Metreon metallographic method and carved accompanying Keller's acid-base indicator. Samples for broadcast power microscopy were cut utilizing wire EDM from miscellaneous zones of the 25 milli metre-dense disagreement stir welded plates [20]. Plate samples were acquired utilizing strand EDM after a ballistic

experiment. Microstructural changes were checked utilizing a light microscope, while rupture morphologies were examined utilizing a high determination scouring power microscope.

## 3 Observation

Before transporting the ballistics tests, the microstructure and machinelike traits of two together the friction stir weld joints and the base material, AA7075-T651, were checked. This reasoning proposed to believe the properties of the fabrics superior to rule bureaucracy to ballistic impact.

The experimental experiment was completed activity to determine the ballistic conducted in 25 milli metre dense plates containing the AA7075-T651 BM. The plates were endangered bullets accompanying lead cores and steel cores, simulating various synopsises. The purpose of these tests searches to judge in what way or manner the fabrics would respond to impact and infiltration by bullets of variable arrangements.

Furthermore, exertions were created to investigate the post-ballistic traits of the checked matters. This contained testing some modifications to the microstructure and microhardness of the regions forthcoming the pierced field. By resolving these post-ballistic traits, analysts aimed to gain intuitions into the material's action under ballistic impact environments and believe in consideration of changes induced by projectile seepage.

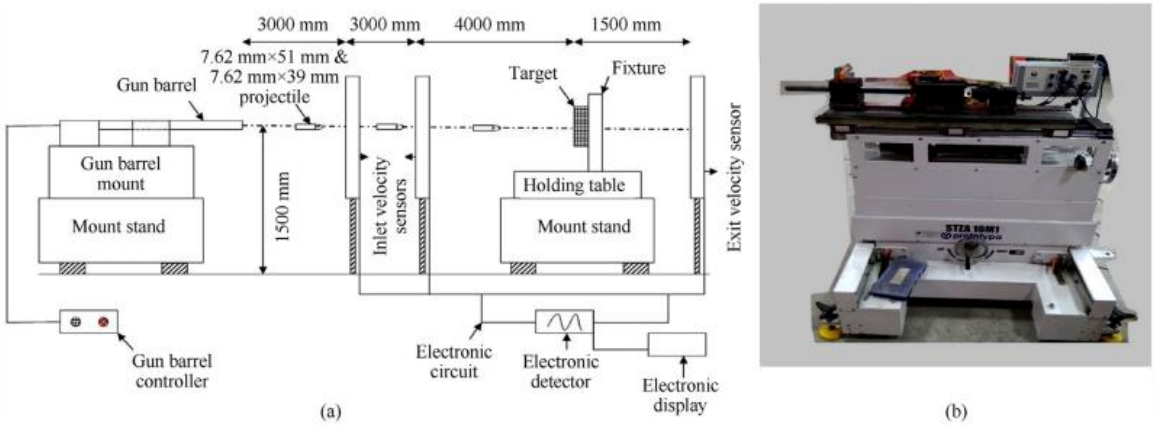


**Figure 2**:*(a) Experimental setup for ballistics tests in diagrammable metric form.; (b) An image depicting an automated gun barrel from a visual perspective.*

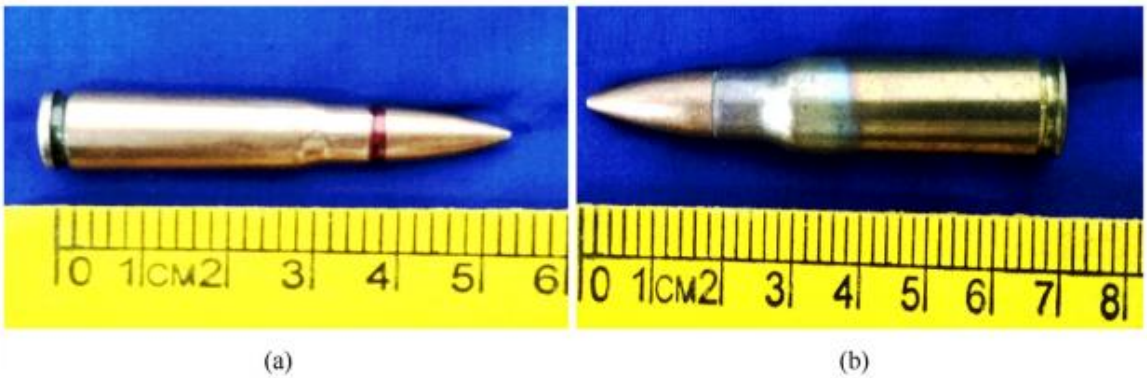


**Figure 3:** *Photographic depiction of projectiles: (a) Steel core projectile (b) Lead core projectile*

Proceedings DOI: 10.21467/proceedings.160
ISBN: 978-81-965621-9-9

Series: AIJR Proceedings
ISSN: 2582-3922

**Table 2:** *The characteristics of the FSW tool which has been used, and the parameters that are involved.*

| Pin Profile | Pin Diameter/mm | Pin Length/mm | Shoulder Diameter/mm | Tool Speed/rpm | Welding Feed Rate/(mm/min) | Tilt Angle/(*) |
|---|---|---|---|---|---|---|
| Taper threaded pin (Left hand metric threads and 1.5 mm pitch) | Bigger End:16 Smaller End:8 | 24.4 | 30 | 150 | 7.5 | 5 |

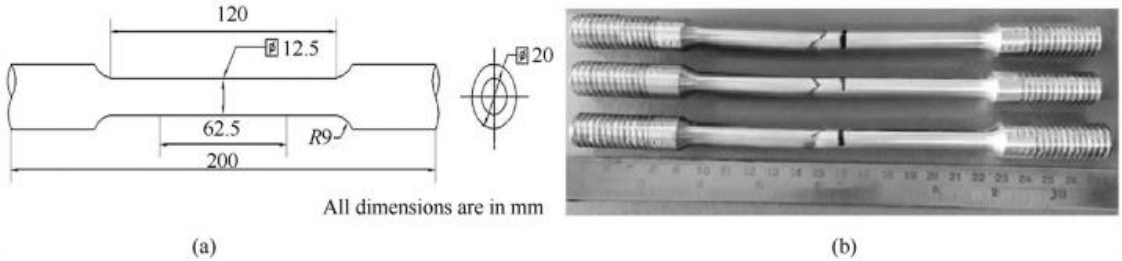


**Figure 4:** *Schematic representation of tensile samples: (a) (2D) geometry of the samples. (b) failed samples*

## 4 Microstructures and Characteristics of FSW Plates

The 25 milli metre plates of AA7075-T651 BM exhibit a microhardness of nearly 175 HV0.5. However, in the bind lump, the microhardness drops to about 105 HV0.5, while in the TMAZ and HAZ, it ranges from 75 to 100 HV0.5. These principles are corresponding to the microhardness of the resolution-medicated material. This desires that the use of reduced pivot speed and very depressed connecting feed all the while Friction Stir Welding (FSW) of AA7075 intersections results in inferior pliable traits at range hotness distinguished to the answer-discussed and T651 base fabrics [21]. The deterioration happens generally in the TMAZ domain. The microhardness principles in the TMAZ, that holds scattered restoring precipitates, can considerably influence the joint substance of the welds. However, despite the lower pliable traits, the impact fighting of the resistance-stir welds is considerably enhanced and distinguished from the base material. This displays that resistance-stir welded plates exhibit reinforced flexibility.

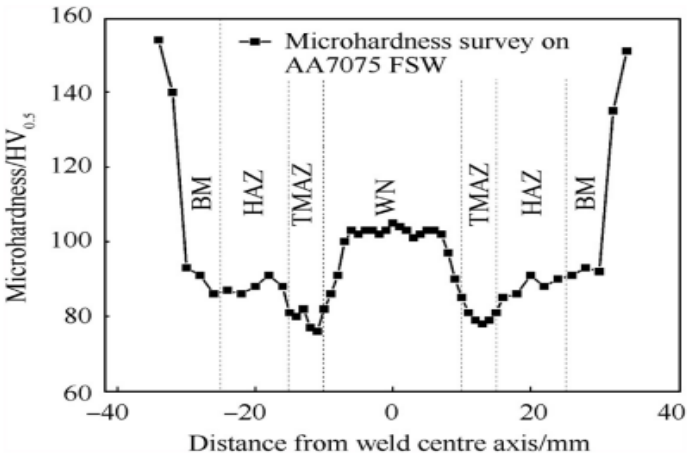


**Figure 5:** *Microhardness profile*

Figure 5 presents a calculating and micro-graphical interpretation of the AA7075-T651 FSW joints, emphasising the base material and differing bind zones [22]. In Figure 6(a), the macrograph of the stir district discloses a dimensional concave makeup accompanying complete infiltration. Figure 6(b) describes the micrograph of the base material, appearance lengthened and pancake-formed grains in the rolling management. Figure 6(c) exhibits equiaxed fine recrystallized grains that are evenly delivered during the whole of the microstructure of the lump zone [23]. Figure 6 (d) explains the closeness of a connected domain between the lump district and the thermos mechanically jolted district, signifying their closeness. Microstructure of the thermomechanical affected district (TMAZ), as noticed in Figure 6(e), exhibits distorted and slanted grains precipitated by the apiece tool's moving motion. Lastly, Figure 6(f) displays the microstructures in the heat-distressed district (HAZ), from lengthened grains familiarize parallel to the width course.

**Table 3:** *Mechanical properties of base plates.*

| Properties/Material | YS/MPa | UTS/MPa | Elongation/% | Joint Efficiency/% | Failure Location | Impact Toughness |
|---|---|---|---|---|---|---|
| BM | 537 ± 6 | 588 ± 6 | 12 ± 3 | - | - | 8 ± 3 |
| FSW | 152 ± 3 | 288 ± 6 | 3.3 ± 3 | 38.78 | TMAZ | 14 ± 3 |

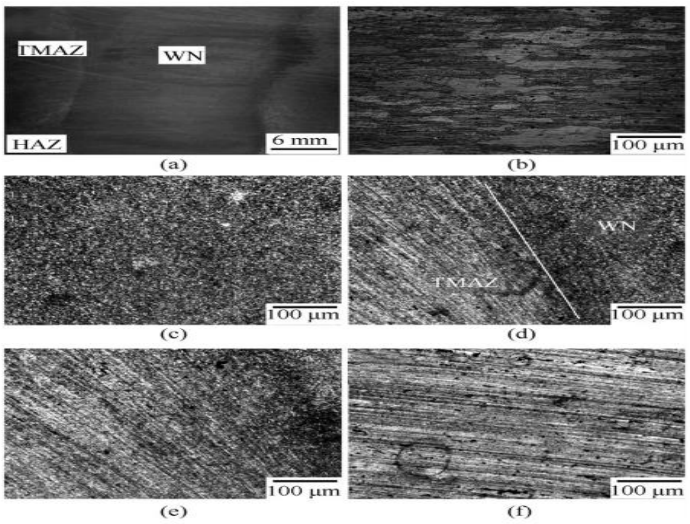


**Figure 6:** *Macro and micrographs*

Figure 7 represents the Transmission Electron Microscope (TEM) concepts of the AA7075-T651 base material and various zones of the FSW in the 25-millimetre-thick plates. The TEM micrograph of the base material (Figure 7a) describes the uniform and thick allocation of strengthening precipitates near the seed borders. However, as heat is used in the weld nugget zone, solid destruction of precipitates happens, developing in a conspicuous break (Figure 7b) [24]. The finish tilt stir causes harsh deformity and decomposition of the grains in the thermo-mechanically affected zone (TMAZ), leading to the rise of minute pieces (Figure 7c). While the classification of precipitates in the heat-affected zone (HAZ) is corresponding to that of the BM, Figure 7d discloses the composition of a speed-free district (PFZ) near the piece horizon on account of the extreme heat recompile.

Proceedings DOI: 10.21467/proceedings.160
ISBN: 978-81-965621-9-9

Series: AIJR Proceedings
ISSN: 2582-3922

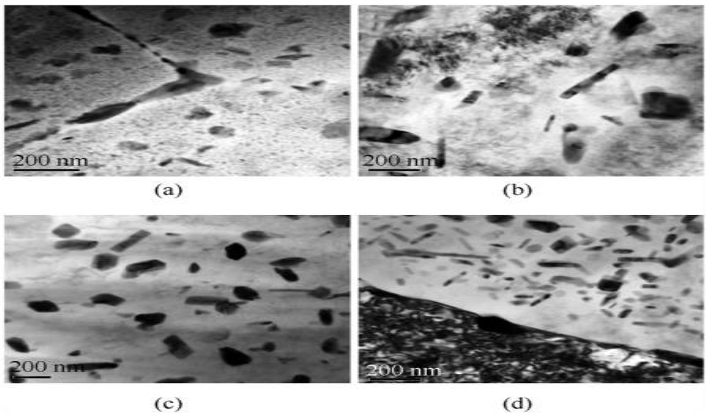


**Figure 7:** *TEM micrographs of 4 zones*

## 5 Ballistic Trials on FSW Plates

The ballistic experiment was attended on the BM and three connect zones of 25 milli metre-dense AA7075-T651 FSW targets. The bullets second-hand in the tests had deformable lead cores weighing 7.62 milli metre and 51 milli metre, in addition to hard fortify cores weighing 7.62 milli metre and 39 milli metre. The impact velocities for the tests were judged 830 ± 20 m/s and 700 ± 30 m/s.

The marks second-hand in the ballistics tests were containing the 25 milli metre-thick AA7075-T651 base material, and two together types of bullets (lead centre and brace core) incompletely pierced the marks. Figures 8(a)-8(c) and Figures 9(a)-9(c) describe the aftermath of bullet impact, disclosing meaningful damage to the goals characterized by material splitting, the composition of uneven-formed cavities, and the invention of cavity obstruction ahead of the central edges of the impact zones (c).

In the case of the lead core bullet, two together the external covering and core material knowing solid deformity and decomposition due to the mark's harder surface distinguished from the bullets themselves. Conversely, the steel centre projectile's centre material pierced the target while only the exposed covering endured damage. Partial infiltration of the bullet was observed. Notably, the lead centre bullet provoked important deformation, as proved in Figs. 8(d) and 8(e), in the connect lump district of the 25 milli metre-thick AA7075-T651 rubbing stir connect goals, developing in the formation of a cauldron-formed crater (f). As described in Figs. 9(d) and 9(e), the steel centre pellet entirely pierced the aim and became entrenched inside it (f). This complete infiltration and implanting of the projectile happen in the thermo-automatically concerned district (TMAZ) of 25 milli metre-thick AA7075-T651 FSW targets, owing to the reduced surface severity of the goal material. These remarks are pictorial in Figures. 8 (g) – 8 (i) and Figs. 9 (g) – 9 (i).

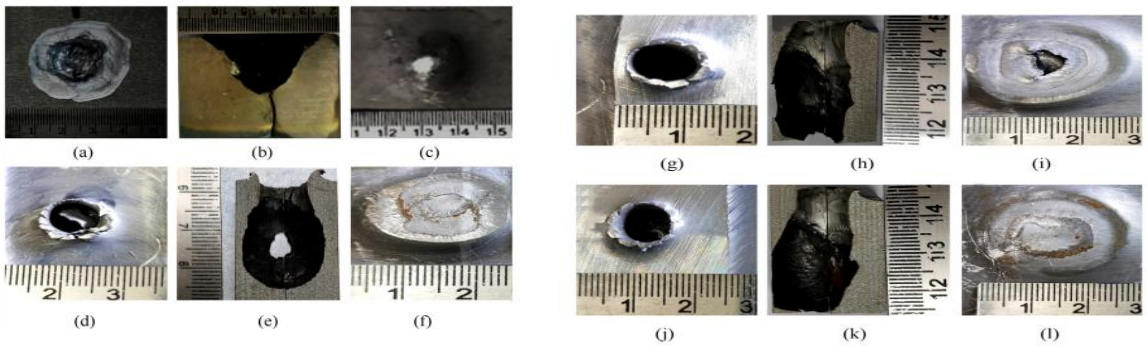


**Figure 8:** *Front, cross-sectioned and rear views with lead core projectile: (a)-(c) BM (d)-(f) Weld Nugget; (g)-(i)-TMZ; (j)-(l) HAZ*

In the haz of the 25 milli metre-dense AA7075-T651 friction stir weld marks, The projectile showed biased shrill at a prone angle, developing in the establishment of a crater inside the heat-concerned district of the marks [26]. The severe deformity was noticed in the case of the lead core projectile, as described in Figs. 8(j)-8(l). Conversely, the steel core bullet sufficiently pierced the goal at a prone angle and enhanced entrenched inside it, as proved in Figs. 9(j)-9(l).

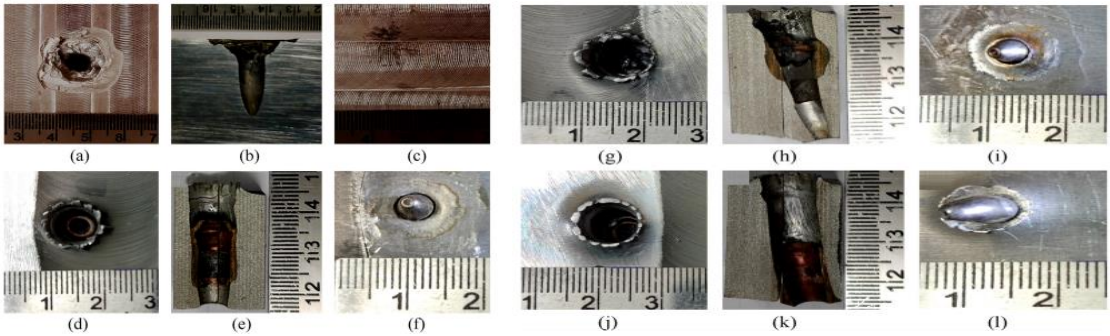


**Figure 9:** *Front, cross-sectioned and rear views (a)-(c) BM; (d)-(f) WN; (g)-(i) TMAZ; (j)-(l) HAZ*

The fracture study revealed that the disappointment trend in the base material was fragile, from material smashing. However, as whole zones of the disagreement stir-welded aims, a flexible fashion of bankruptcy was noticed, from the establishment of petalling at the front followed by flexible dent increase. Petalling refers to the deformity pattern that happens when a hemispherical or cylindrical bullet impacts a material. Surface petalling is affected by apiece impact speed [24]. In the case of the lead centre bullet, two together the base materials as well FSW goal zones show a bulge on the rear face of the goal.

## 6 Target's Post-Ballistic Characteristics

Figure 10 displays the scanning electron microscopy of the base material in addition to zones of the FSW samples that met with the ballistic experiment. In Figure 10(a), the fractography of the base material discloses craters accompanying soften parts and the lack of dimples. This displays that the fad of bankruptcy in the samples was fragile.

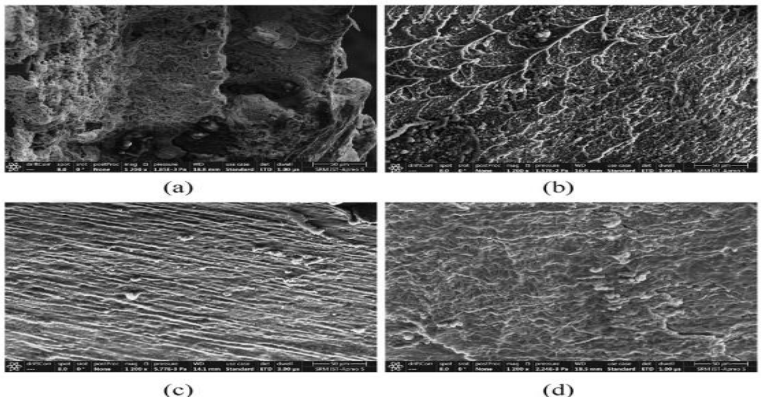


**Figure 10:** *SEM fractographs (a) BM (b) WN (c) TMAZ (d) HAZ*

Figure 10 displays that the operation of the form stir completely restructured the grains in the bind lump zones, developing in revised ductility of the material and raising opposition against bullet infiltration (b). The tool stir operation managed the composition of abundant, plastically deformed grains accompanying separated precipitates. In the thermo-mechanically affected zone (TMAZ), the deformed grains bent on the way to the connection, admitting bullets to pass through more surely. The TMAZ was erect and expected the softest district based on the severity survey bestowed in Figure 5. Figure 10(c) supplies a clear model of material laceration made by ball infiltration. While the heat-afflicted district (HAZ) contributes a little

Proceedings DOI: 10.21467/proceedings.160
ISBN: 978-81-965621-9-9

Series: AIJR Proceedings
ISSN: 2582-3922

opposition against bullet seepage, the development of speed-free zones near seed bounds significantly reduces frictional fighting and leads to intergranular fractures, founding a subordinate weak area in the weld (Figure 10(d)). In the denseness course expected the fields place the bullets pierced, a microhardness study was accompanied on the cross-separate Camille metre infiltration channel. Figures 11(a) and 11(b) embellish the post-ballistic microhardness survey of 25 milli metre-thick AA7075-T651 FSW samples subjected to lead meaning and encircle centre bullets. The Figures reveal the changeable microhardness standard in the separate zones of the friction stir-welded AA7075-T651 material and the fundamental BM.

**Table 4:** *Results of experimental ballistics tests using targets made of friction stir-welded 25 milli metre-thick AA7075-T651 base material*

| S.no | Weld zone | Projectile core type | Initial velocity(m/s) | Hole diameter/mm | | Depth of penetration | Inference |
|---|---|---|---|---|---|---|---|
| | | | | Front side | Back side | | |
| 1 | BM | Lead | 851 | 19.5 | - | 15 | PP |
| 2 | | Steel | 704 | 24.5 | - | 19 | PP |
| 3 | WN | Lead | 840 | 12 | - | 10 | PP |
| 4 | | Steel | 709 | 10 | 4 | 25 | CP&E |
| 5 | TMAZ | Lead | 845 | 13 | 4 | 25 | PP |
| 6 | | Steel | 703 | 10 | 5 | 25 | CP&E |
| 7 | HAZ | Lead | 847 | 11 | - | 23 | PP |
| 8 | | Steel | 705 | 10 | 8 | 25 | CP&E |

*PP – Partial penetration *CP&E – Complete and embedment

Figure 11 presents targets before following in position or time impact accompanying a lead gist shot (a). The average severity principles of the base material were persistent expected 175 HV0.5 before impact and 180 HV0.5 after impact. The average severity principles in the weld nugget (WN) zone were erect expecting 105 HV0.5 before impact and 120 HV0.5 following in position or time impact. Similarly, the average severity principles in the thermo-automatically overwhelmed district (TMAZ) were 85 HV0.5 before impact and 98 HV0.5 afterwards impact. For the heat-damaged district (HAZ), the average severity principles were 75 HV0.5 before impact and 85 HV0.5 after impact. Regarding impact accompanying a steel core projectile, Figure 11(b) exemplifies the variable microhardness principles in different zones of the rubbing stir-welded AA7075-T651 aims. The average severity principles of the base material were driven expecting 175 HV0.5 before impact and 180 HV0.5 subsequently after impact. The average severity principles in the WN district were found expected 105 HV0.5 before impact and 125 HV0.5 afterwards impact. The average severity principles in the TMAZ were 85 HV0.5 before impact and 100 HV0.5 subsequently after impact. In the HAZ, the average severity principles were 75 HV0.5 before impact and 125 HV0.5 afterwards impact. The increase in surface hardness of all the 3 zones is accredited to the wantonness of bullet moving power in the goal, which results in the deformity of internal piece forms and piece cultivation in the domain pierced for one bullet, chief to strain thickening. However, when an aim or bullet maintains meaningful damage, outside conspicuous changes in severity principles, it indicates the entertainment of the bullet moving power into the material. Steel gist bullets exhibit a roomier range of severity principles distinguished to lead core bullets in the judged 25 milli metre-dense disagreement stir-welded AA7075-T651 aims for the ballistic experiment. Bottom of Form

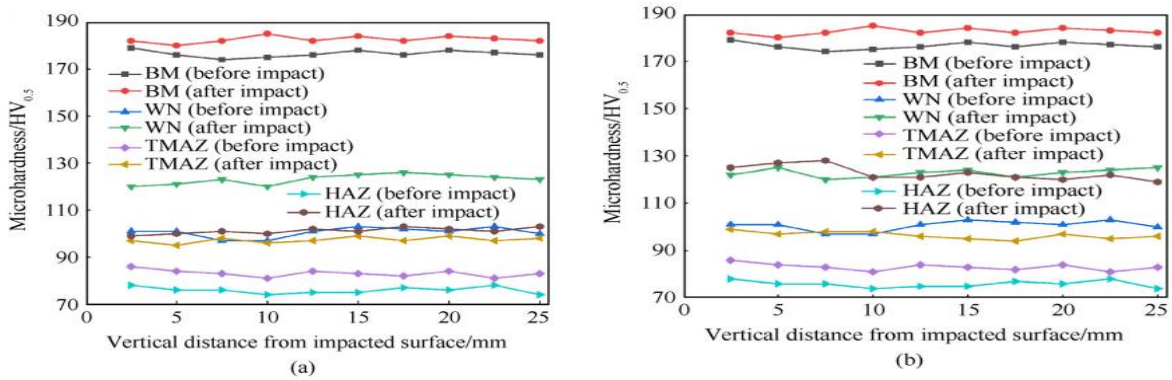


**Figure 11:** *Microhardness survey: (a) Lead core projectile; (b) Steel core projectile*

As the projectiles began the penetration zone, there were apparent changes in the micrographs. Figures 12-15 describe the post-ballistic micrographs of three unconnected zones (WN, TMAZ, and HAZ) in AA7075-T651 FSW aims at a 25-milli metre BM. In Figures 12 and 13, the micrographs of the BM and WN zones for ballistic against two together lead centre and steel gist bullets positively manifest that skilled were no conspicuous alterations in these zones.

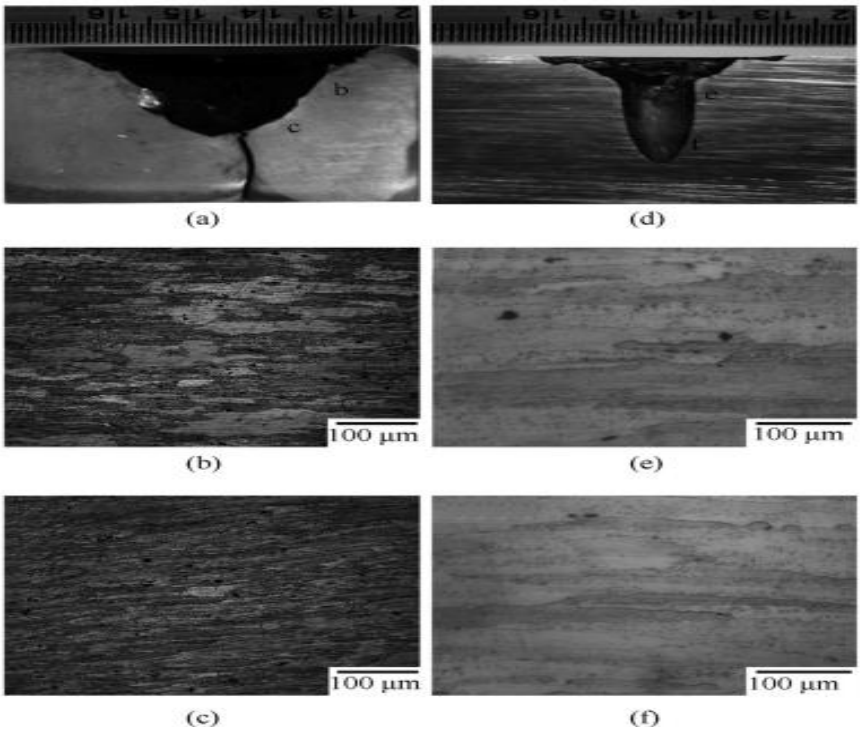


**Figure 12:** *Micrographs: Base material (a)e(c) lead core projectile and (d)e(f) steel core projectile*

Proceedings DOI: 10.21467/proceedings.160
ISBN: 978-81-965621-9-9

Series: AIJR Proceedings
ISSN: 2582-3922

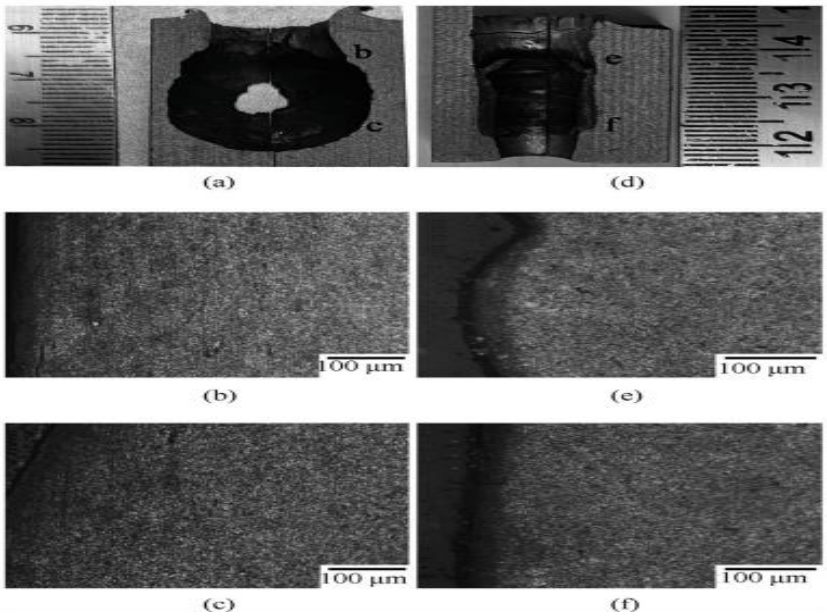


**Figure 13:** *Micrographs: FSW Weld Nugget (a)e(c) lead core projectile and (d)e(f) steel core projectile*

Figures 14 and 15 manifest observable alterations in the micrographs forthcoming the fields pierced by the bullets. These alterations involve grain reorganization, the establishment of adiabatic cut bands (ASB), and significant grain deformation resulting in bends along the route of bullet seepage [25]. ASB serves as better sites that the introduction and procreation of micro-voids and fractures under vital stresses, someday chief to material failure [27]. The noticed piece deformity in the examined samples climaxes the relationship between changes in severity principles and the microstructures. [20-22].

Shear stress, $\tau = (\tau_0 + h\gamma)e^{\{-\frac{\eta\alpha\gamma}{2\rho C}(2\tau_0+h\gamma)\}}$ (1)

Temperature rise, $\theta = \frac{1}{\alpha}\left\{1 - e^{\left[-\frac{\eta\alpha\gamma}{2\rho C}(2\tau_0+h\gamma)\right]}\right\}$ (2)

where, t = shear stress (MPa), q = temperature rise (K), $t_0$ = shear proportion limit (MPa), h = strain hardening coefficient (GPa), $\alpha$ = thermal softening coefficient (K), $\eta$ = thermal transition coefficient, $\gamma$= density (kg/m3), c = specific heat capacity (J/kg.K).

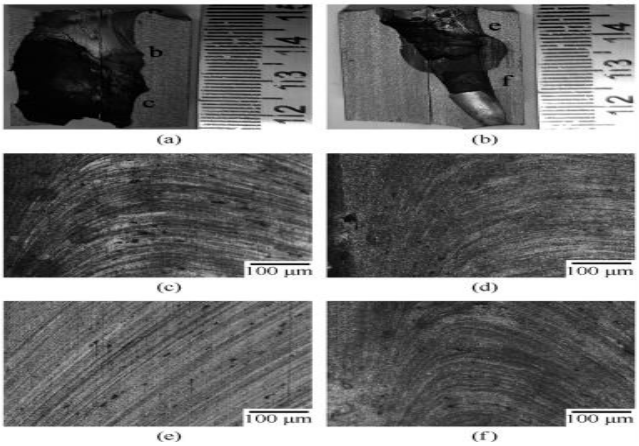


**Figure 14:** Micrographs on ballistic proven 25 milli metre steel core projectile.

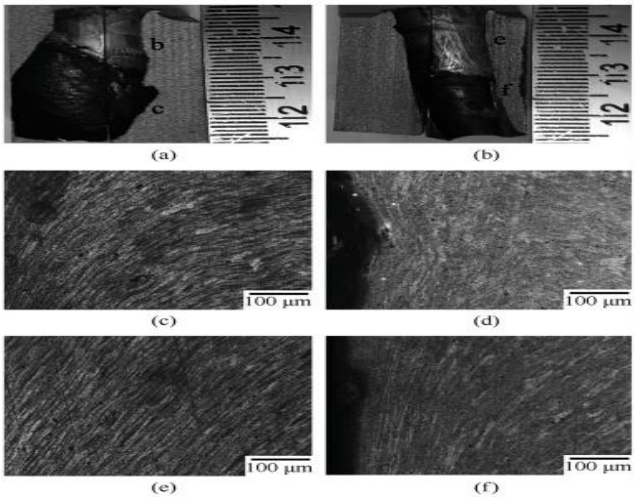


**Figure 15:** *Micrographs on ballistic proven 25 milli steel core bullet*

In Table 5, the variables and constants used for finding the shear stress and temperature increase for the AA7075-T651 material are provided [28]. When these values are plugged into the equation mentioned, the shear stress when the formation of adiabatic shear bands under dynamic loading conditions is determined to be 2120 MPa, while the corresponding temperature increase is calculated to be 791 K.

## 7 Conclusion

After transporting all the ballistic experiments, the following decisions were drawn from the extreme-speed bullet impact tests performed on 25 milli metre dense joined plates of AA7075-T651 BM and miscellaneous zones of FSW aims against lead centre bullets and hardened steel centre bullets:

1. The BM and FSW goals showed meaningful damage upon projectile impact, containing material riving, irregular-formed crater composition, and crater obstruction explanation.

2. The lead gist projectiles have knowledgeable deformity and decomposition of their outer covering and centre material, while the steel gist bullets generally penetrated the goals accompanying only damage to their exposed casing.

3. In the bind lump district of friction stir-welded aims, the lead centre projectiles formed cauldron-formed cavities on account of harsh deformity, while the steel gist bullets adequately penetrated and abided themselves in the aims.

Proceedings DOI: 10.21467/proceedings.160
ISBN: 978-81-965621-9-9

Series: AIJR Proceedings
ISSN: 2582-3922

4. The TMAZ of friction stir-welded marks, accompanying lowered surface hardness, admitted the lead gist and fortified core bullets to pierce and sink themselves in the targets.

5. Fracture in the base material happens in a tense mode accompanying material splitting, while all zones of the disagreement stir-welded targets show a flexible manner of failure accompanying front petalling establishment and after ductile dent increase.

6. The hardness survey demonstrated that the TMAZ had the softest district, providing easier bullet seepage.

7. The incident of adiabatic shear bands (ASBs) and important piece deformity were observed forthcoming the extents penetrated apiece bullet, superior to changes in microstructures and hardness principles.

8. The wantonness of bullet kinetic energy through deformity of within piece structures and strain thickening donated to enhanced mark surface severity effectively three separate zones.

9. Steel core bullets show a roomier range of hardness principles distinguished to lead gist projectiles in resistance stir-welded aims of AA7075-T651 material.

The AA7075-T651 is usually a metallic alloy accompanying distinguishing specifications and perpetual principles. Here are a few of Allure's key requirements:

1. Composition: The AA7075-T651 alloy generally consists of usually metallic (Al) as the base factor, in addition to percentages of added alloying elements. The typical composition is nearly Al, zinc (Zn), magnesium (Mg), and copper (Cu) are 90.7%, 5.6%, 2.5% and small amounts of different parts.

2. Heat Treatment: The "T651" label displays that the alloy has sustained a resolution heat treatment trailed by affected maturing. This heat situation process improves the material's mechanical properties, containing substance and severity.

3. Thickness: The ballistics tests and notes noticed a thickness of 25 millimetres for the AA7075-T651 plates. This signifies that the material was judged and resolved in a 25-milli metre-girth arrangement.

4. Shear Stress and Temperature Increase: Table 5, noticed in a previous statement, holds the variables and limit used to decide the cut stress and hotness increase for the AA7075-T651 material. These values are hopeful particular to the exploratory arrangement and experiment conditions. It is main to note that distinguishing qualifications and determined principles can change depending on the maker, result principles, and heat required to raise temperature situation processes second-hand.

Therefore, it is advisable to concern the appropriate mechanics proof or confer material requirements from reliable beginnings for precise and current news on AA7075-T651 alloy characteristics.

**Table 5:** *Change in the characteristics of the welded AA7075-T61 plates on striking with steel and iron core bullet*

| $\tau_0 = \sigma_0/2$/MPa | h/GPa | α/K | η | ρ/(kg.mm3) | c/(J.k/kg) |
|---|---|---|---|---|---|
| 384 | 4 | 1/1273 | 0.9 | 2840 | 1005 |

The detailed decision for the change in the characteristics of the welded AA7075-T61 plates on striking with steel and iron core bullets by way of the ballistics tests are given beneath:-

1. In 25 milli metre-thick AA7075-T651 plates (BM), the lead-core projectile pierces to an insight of almost 15 milli metre, while the steel-core pellet pierces to an insight of about 19 milli metre. In diversified zones of difference stir welded samples, the infiltration wisdom for lead-gist shots are almost WN, HAZ, and TMAZ (20milli metre, 23milli metre, 25milli metre ), while for gird-gist bullets, the insights are WN-25 milli metre, HAZ, TMAZ(25milli metre, 25 milli metre). Although the shot reinforces established in the material when the leakage insight reaches 25 milli metre, no prick occurs in individual these cases. This cataclysm ratifies the veracity of requesting AA7075-T651 resistance stir welds on 25 milli metre-dense plates in ballistic constructions and bulletproof automobiles.
2. In the BM, it is spall fragmentation, signifying fragile deterioration accompanying lower penetration insights. However, front pedalling, from smooth bullet seepage and embedment, was noticed in the various zones of FSW, suggesting pliant collapse accompanying better penetration wisdom.
3. A microhardness survey transported on ballistically proven samples told no meaningful hardness changes in the base material in the bullet-penetrated region. However, notable dissimilarities in severity were observed entirely in zones of friction stir weld. This is generally accredited work thickening, which happens as the bullets' moving power disappears into the aims through compression stresses on the bullet-cut extents.
4. Similarly, no solid severity changes were found in the base material in the bullet-penetrated field, as pointed out by a microhardness survey. However, important differences in severity were noticed comprehensively in zones of resistance stir welds. This may be attributed to work thickening provoking apiece disappearance of moving power from the projectiles into the targets, happening in condensation stresses on the bullet-penetrated areas.

Based on the remarks and judgments fatigued from the ballistic experiments on AA7075-T651 FSW, it may be implicit that this material exhibits good characteristics distinguished to brace when used in combat cabs. Some indispensable content advocating this declaration contains:

1. Penetration Depth: The AA7075-T651 material showed greater resistance to penetration by lead-core and steel-core bullets distinguished from steel. This signifies that the material supplies better guardianship against ballistic threats, conceivably embellishing the overall substance and survivability of combat vehicles.
2. Failure Mechanism: The noticed ductile defeat in the miscellaneous zones of disagreement stir welds desires that the AA7075-T651 material can consume and expend the kinetic energy from bullets in a more excellent manner, lowering the risk of destructive decline. In contrast, the base material (steel) showed fragile breakdown, signifying a taller susceptibility to spall decomposition and material disintegration.
3. Hardness Changes: The meaningful distinctness's in severity noticed in the friction stir bind zones signify that the AA7075-T651 material sees work thickening when Comilla metre ballistic impacts. This suggests that the material can better bear and consume the strength from bullets, providing raised opposition to deformation and potential infiltration.

Based on these verdicts, it may be decided that the use of AA7075-T651 in combat jeeps offers improved features distinguished to fortify, providing improved substance, durability, and guardianship against ballistic threats. However, it is main to believe added determinants such as pressure, cost, and particular use necessities when selecting fabrics for combat vehicle explanation.

Proceedings DOI: 10.21467/proceedings.160
ISBN: 978-81-965621-9-9

Series: AIJR Proceedings
ISSN: 2582-3922

## 8 Publisher's Note

AIJR remains neutral with regard to jurisdictional claims in institutional affiliations.

## How to Cite

Kumar & Narayana (2023). The use of AA7075-T651 Alloy in Combat Vehicles Offers Superior Properties Compared to Steel, Providing Enhanced Strength and Durability: A Review. *AIJR Proceedings*, 481-496. https://doi.org/10.21467/proceedings.160.61

## References

[1] Erdem M, Cinici H, Gokmen U, Karakoc H, Turker M. Mechanical and ballistic properties of powder metal 7039 aluminium alloy joined by friction stir welding. Trans Nonferrous Met Soc China (English Ed) 2016;26(1):74e84. https://doi.org/10.1016/S1003-6326(16)64090-6.

[2] Rao TS, Reddy GM, Rao GS, Rao SRK. Studies on salt fog corrosion behaviour of FSW AA7075-T651 aluminium alloy. Int J Mater Res 2014;105(4):375e85. https://doi.org/10.3139/146.111033.

[3] Li D, Yang X, Cui L, He F, Zhang X. Investigation of stationary shoulder friction stir welding of aluminium alloy 7075-T651. J Mater Process Technol 2015;222: 391e8. https://doi.org/10.1016/j.jmatprotec.2015.03.036.

[4] Sivaraj P, Kanagarajan D, Balasubramanian V. Effect of post weld heat treatment on tensile properties and microstructure characteristics of friction stir welded armour grade AA7075-T651 aluminium alloy. Def Technol 2014;10(1):1e8. https://doi.org/10.1016/j.dt.2014.01.004.

[5] Kumar PV, Reddy GM, Rao KS. Microstructure, mechanical and corrosion behaviour of high strength AA7075 aluminium alloy FSW e effect of post weld heat treatment. Def Technol 2015;11(4):362e9. https://doi.org/10.1016/j.dt.2015.04.003.

[6] Rao TS, Reddy GM, Rao SRK. Microstructure and mechanical properties of FSW AA7075-T651 aluminium alloy thick plates. Trans Nonferrous Met Soc China (English Ed) 2015;25(6):1770e8. https://doi.org/10.1016/S1003-6326(15)63782-7.

[7] Azimzadegan T, Serajzadeh S. An investigation into microstructures and mechanical properties of AA7075-T6 during friction stir welding at relatively high rotational speeds. J Mater Eng Perform 2010;19(9):1256e63. https://doi.org/10.1007/s11665-010-9625-1.

[8] Rao TS, Rao SRK, Reddy GM. Microstructure and fracturing behaviour of AA7075eT651 aluminium alloy Cooled during friction stir welding. Met Sci Heat Treat 2019;61(5e6):379e86. https://doi.org/10.1007/s11041-019-00433-y.

[9] Meng X, Huang Y, Cao J, Shen J, dos Santos JF. Recent progress on control strategies for inherent issues in friction stir welding. Prog Mater Sci 2021;115:100706. https://doi.org/10.1016/j.pmatsci.2020.100706.

[10] Mishra RS, Ma ZY. Friction stirs welding and processing. Mater Sci Eng R Rep 2005;50(1e2):1e78. https://doi.org/10.1016/j.mser.2005.07.001.

[11] Jung J, Cho YJ, Kim SH, Lee YS, Kim HJ, Lim CY, et al. Microstructural and mechanical responses of various aluminium alloys to ballistic impacts by ar more piercing projectile. Mater Char 2020;159:110033. https://doi.org/10.1016/j.matchar.2019.110033.

[12] Sudhakar I, Madhusudhan Reddy G, Srinivasa Rao K. Ballistic behaviour of boron carbide reinforced AA7075 aluminium alloy using friction stir processing e an experimental study and analytical approach. Def Technol 2016;12(1):25e31. https://doi.org/10.1016/j.dt.2015.04.005.

[13] Khan MA, Wang Y, Cheng H, Yasin G, Malik A, Nazeer F, et al. Microstructure evolution of an artificially aged Al-Zn-Mg-Cu alloy subjected to soft- and hard-steel core projectiles. J Mater Res Technol 2020;9(5):11980e92. https://doi.org/10.1016/j.jmrt.2020.08.076.

[14] Übeyli M, Balci E, Sarikan B, Oztas € ¸ MK, Camus¸ cu N, Yildirim RO, et al. The ballistic performance of SiC-AA7075 functionally graded composite produced by powder metallurgy. Mater Des 2014;56:31e6. https://doi.org/10.1016/j.matdes.2013.10.092.

[15] Mondal C, Mishra B, Jena PK, Siva Kumar K, Bhat TB. Effect of heat treatment on the behaviour of an AA7055 aluminium alloy during ballistic impact. Int J Impact Eng 2011;38(8e9):745e54. https://doi.org/10.1016/j.ijimpeng.2011.03.001.

[16] Børvik T, Hopperstad OS, Pedersen KO. Quasi-brittle fracture during the structural impact of AA7075-T651 aluminium plates. Int J Impact Eng 2010;37(5): 537e51. https://doi.org/10.1016/j.ijimpeng.2009.11.001.

[17] Fras T, Collard L, Lach E, Rusinek A, Reck B. Thick AA7020-T651 plates under The ballistic impact of fragment-simulating projectiles. Int J Impact Eng 2015;86: 336e53. https://doi.org/10.1016/j.ijimpeng.2015.08.001.

[18] Pedersen KO, Børvik T, Hopperstad OS. Fracture mechanisms of aluminium alloy AA7075-T651 under various loading conditions. Mater Des 2011;32(1):97e107. https://doi.org/10.1016/j.matdes.2010.06.029.

[19] Ma X, Meng X, Xie Y, Zhao Y, Peng X, Liang M, Mao D, Wan L, Huang Y. Elimination of root kissing bond in friction stirs welding of thick plates. Mater Lett 2022;328:133148. https://doi.org/10.1016/j.matlet.2022.133148.

[20] Praveen R, Koteswara Rao SR, Damodaram R, Suresh Kumar S. Numerical and experimental investigations on the effect of target thickness and solution treatment on the ballistic behaviour of AA7075 thick plates. Proc IME C J Mech Eng Sci 2022;236(7):3530e45. https://doi.org/10.1177/09544062211038981.

[21] Praveen R, Rao SK, Kumar SS, Babu TR. Numerical evaluation of ballistic limit velocity and the experimental ballistic response of 25 milli metre-thick aluminium 7075 alloy targets. Mater Today Proc 2022;62(2):523e9. https://doi.org/10.1016/ j.matpr.2022.03.587.

[22] Praveen R, Koteswara Rao SR, Kumar SS, Suresh Kumar S. Optimization of target thickness and investigation of the effect of heat treatment on the ballistic performance of aluminium alloy 7075 targets against hard steel core projectile. Proc IME J Mater Des Appl

2023;237(1):131e43. https://doi.org/10.1177/14644207221105365.

[23] Srinivasa Rao T. Friction stirs welding of AA 7075 thick plates: evaluation of mechanical and corrosion behaviour. Thesis. Chennai: Anna University; 2015.

[24] Wierzbicki T. Petalling of plates under explosive and impact loading. International. Int J Impact Eng 1999;22(9e10):935e54. https://doi.org/10.1016/S0734-743X(99)00028-7.

[25] Lee CG, Lee Y-J, Lee S. Observation of adiabatic shear bands formed by ballistic impact in aluminium-lithium alloys. Scripta Metall Mater 1995;32(6):821e6. https://doi.org/10.1016/0956-716X(95)93208-L.

[26] Xu YB, Zhong WL, Chen YJ, Shen LT, Liu Q, Bai YL, et al. Shear localization and recrystallization in dynamic deformation of 8090 AleLi alloy. Mater Sci Eng A 2001;299(1):287e95. https://doi.org/10.1016/S0921-5093(00)01412-X.

[27] Li Q, Xu YB, Lai ZH, Shen LT, Bai YL. Dynamic recrystallization induced by plastic deformation at a high strain rate in a Monel alloy. Mater Sci Eng A 2000;276(1):250e6. https://doi.org/10.1016/S0921-5093(99)00127-6.

[28] De Maddis M, Russo Spena P. Plastic flow behaviour of twinning induced plasticity steel from low to warm temperatures. J Mater Res Technol 2020;9(2):1708e19. https://doi.org/10.1016/j.jmrt.2019.11.09

Proceedings DOI: 10.21467/proceedings.160
ISBN: 978-81-965621-9-9

Series: AIJR Proceedings
ISSN: 2582-3922